Semiconductor Physics, Quantum Electronics & Optoelectronics, 2025. V. 28, No 2. P. 232-238.

Optoelectronics and optoelectronic devices

Flash lamp annealing of $Cu(In_{1-x}Ga_x)SSe$ films deposited on polyimide substrate: Crystalline structure and chemical composition

I.P. Tyagulski[1], O.Yo. Gudymenko[1], A.V. Rusavsky[1], S.I. Tiagulskyi[2], O.F. Isaieva[1], S.V. Kondratenko[3], V.S. Lysenko[1], D. Flandre[4], A.N. Nazarov[1,5]

[1]*V. Lashkaryov Institute of Semiconductor Physics, NAS of Ukraine, Kyiv, Ukraine*
[2]*Institute of Photonics and Electronics of the Czech Academy of Sciences, Prague, Czech Republic*
[3]*Taras Shevchenko National University of Kyiv, Kyiv, Ukraine*
[4]*ICTEAM, UCLouvain, Louvain-la-Neuve, Belgium*
[5]*National Technical University of Ukraine "Igor Sikorsky Kyiv Polytechnic Institute", Kyiv, Ukraine*
[*]*Corresponding author e-mail: nazarov@lab15.kiev.ua*

Abstract. In this paper, the effect of sub-millisecond range flash lamp annealing (FLA) on the microstructural and chemical composition of copper indium gallium selenide sulfide (CIGSS) films deposited at low temperature (below 350 °C) on flexible polyimide was studied. The results of scanning electron microscopy (SEM), X-ray diffraction (XRD), and micro-Raman spectroscopy indicate that flash lamp annealing leads to a more homogeneous polycrystalline structure and reduces the defect concentration in the CIGSS layer. Additionally, energy-dispersive X-ray spectroscopic (EDS) measurements show that copper concentration slightly increases, with a slight decrease in the concentration of Ga and In.

Keywords: flash lamp annealing, scanning electron microscopy, X-ray diffraction, micro-Raman spectroscopy.

https://doi.org/10.15407/spqeo28.02.232
PACS 61.05.cp, 81.40.Ef, 88.40.jn

Manuscript received 10.01.25; revised version received 07.04.25; accepted for publication 11.06.25; published online 26.06.25.

1. Introduction

Flexible and stretchable electronics is a highly multi-disciplinary research area with the potential for significant breakthroughs in developing new technologies for both ubiquitous and unique electronics [1], for example, on-skin electronics. The creation of solar cells on flexible substrates requires special low-temperature treatments to obtain qualitative photo-absorbing material. Photo-absorbers, namely $Cu(InGa)Se_2$ (CIGS) or Cu(InGa)SSe (CIGSS), are very promising for fabricating solar cells on flexible wafers.

As noted in literature from 2024, the efficiency of these solar cells on glass substrate produced by Solar Frontier (Japan) and tested by AIST (Japan) reached 23.35% [2]. The review [5] states that a flexible polyimide (PI) substrate has been considered the most promising candidate for flexible CIGS PV products. CIGS solar cells reached an efficiency of 20.8% on a flexible PI substrate [3]. These record values were attributed to both the low-temperature three-stage co-evaporation process involving heavy alkali elements and post-deposition low-temperature treatment. Additionally, PIs are generally regarded as highly "biocompatible" [4]. Unfortunately, the record cell efficiency [2, 3] is more a "laboratory record" than achievable in the industry. In the industry for PI substrate, the cell efficiency does not exceed 15% [5, 6]. Without a doubt, the methods of annealing the material make significant contributions to the efficiency of the cell.

Regarding this, the paper presents a study of the post-deposition sub-millisecond range flash lamp annealing effect on the microstructural and chemical composition of CIGS films deposited on PI wafer.

2. Experimental part

2.1. Sample preparation

The CIGSS films were deposited using RF plasma magnetron sputtering in an Ar ambient from a granulated $Cu(In_{0.7}Ga_{0.3})SSe$ target (American Elements Co, USA) on molybdenum-coated PI substrates. The temperature of the wafer during magnetron deposition was close to 300 °C. The power of the RF discharge was close to 250 W.

To perform FLA treatment, we have used a modified two-lamp optical head from an impulse ruby laser. Instead of the active element, the sample holder

was placed between two IFP-8000 lamps, and a diffuse reflector was also used. The back surface of the sample (PI substrate) was covered with a white plate. Thus, the irapplied radiation energy was absorbed exclusively by the open surface of the CIGS absorber. By varying the number of capacitors in the storage block (from 100 to 1200 μF), as well as the voltage (up to 3.5 kV), the optimal process parameters were selected. The sub-millisecond annealing mode was applied. It was sufficient to provide annealing in the thermal conductivity regime [7] when annealing occurs mainly in subsurface regions. To prevent destroying the CIGSS film on glass and PI substrates, the energy fluence was within the range of 0.2…0.7 J/cm^2. The phases of FLA treatment were performed sequentially, one by one, and the measurements of structural parameters were carried out between these phases.

2.2. Sample characterization

The morphology of $Cu(In_{1-x}Ga_x)SSe$ layers on polyimide was studied using scanning electron microscopy (SEM, Tescan Lyra 3 GM FIB/SEM), while the elemental microanalysis of CIGSS was carried out using the energy-dispersive X-ray spectroscopy (EDXS, "OXFORD Instruments"). For the microanalysis of transition metal elements, K lines are usually preferred to L lines to avoid chemical effects (*i.e.* change in peak shape and position).

The X-ray structural study was carried out using a Panalytical X'Pert Pro MRD X-ray diffractometer by using the following parameters: CuKαl radiation at λ = 0.15406 nm, the voltage at the tube anode equal to 45 kV, and the current fixed at 40 mA. The diffractograms were obtained using the sliding beam method, the X-ray incident angle was 2 degrees.

Raman measurements were performed at room temperature using a Renishaw 1000 micro-Raman system in a backscattering configuration with a 532 nm excitation laser. A laser spot size close to 3 μm was achieved using a 100× objective. To prevent sample damage and thermal effects, the excitation power did not exceed 5 mW.

3. Results and discussion

3.1. Surface morphology and chemical composition

After RF plasma magnetron deposition, the CIGSS films on the molybdenum layer have a polycrystalline structure with a wide distribution of crystallite sizes (500…2000 nm (Figs. 1a and 1e). The chemical composition of the studied films was slightly different compared to the target: the films were slightly depleted in Ga and Cu (see Table 1).

After the FLA with optimal energy fluence (0.627 J/cm^2) the surface of the CIGSS films becomes more homogenous – grain size is concentrated close to 1300 nm (Fig. 1f) and the film thickness slightly decreased from 2.58 to 2.30 μm (Figs. 1b and 1d). The results of microanalyses confirm the same.

Table 1 shows the quantitative EDXS analysis for $Cu(In_{1-x}Ga_x)SSe$ layers before and after the FLA with optimal fluence (0.627 J/cm^2). The relation of Cu/(In + Ga) after the optimal FLA increases from 82 to 0.87 at.%, which is very close to the stoichiometric value, whereas the relation of Ga/(In + Ga) changes from 26 at.% to 25.6 at.%. The chemical composition of our materials after FLA can be presented as $Cu(In_{0.74}Ga_{0.26})(Se_{0.54}Se_{0.46})_2$.

The relation of Ga/(In + Ga) allows us to calculate the band gap energy (E_g) of our semiconductor material [8] using the following equation:

$$E_g = 1.00 + 0.55\left(\mathrm{Ga}/\left(\mathrm{In}+\mathrm{Ga}\right)\right) + 0.13\left(\mathrm{Ga}/\left(\mathrm{In}+\mathrm{Ga}\right)\right)^2 (\mathrm{eV}).$$

The band gap of our photoabsorber is 1.15 eV (see Table 1), which is close to the optimal value (1.20 eV) obtained using the simulation of the efficiency of the solar cell in [9].

3.2. Structural measurements

The XRD patterns of CIGSS on PI absorber before and after FLA-treatment are shown in Fig. 2. The positions of XRD peaks are very close to the position of the tetragonal phase reflexes of $CuGa_{0.3}In_{0.7}SSe$ (PDF № 000-59-0290) Space Group I-42d. The lattice parameters were calculated using a full-profile analysis by the Rietveld method [10, 11] in the High Score Plus program. The weighted measure of the quality of fitting the theoretically calculated profile to the experimentally obtained diffractogram (Rwp parameter) [11] is no higher than 8.0. According to the fitting methodology, the Rwp parameter should be below 15.0. A change in the lattice parameters is indicated by shifts of reflexes (Fig. 2b). Thus, parameter *a* increases, while parameter *c*, on the contrary, decreases (Table 2).

It is known [12–14] that the reduction of the lattice parameters is due to the increase in the concentrations of Ga and S atoms because their atomic radii are smaller than the atoms they replace (In, Se). This change is linear for both parameters *a* and *c*. After FLA treatment, the concentrations of Ga and In atoms decrease (see Table 1), which can be caused by the following: (1) formation of vacancy defects that lead to a decrease in the *c* parameter [15], (2) relaxation of tensile strain after FLA, which created an excess of Ga and In atoms in the initial state.

The opposite situation is observed with the concentrations of S and Se and their sum (see Table 2). It increases, correspondingly, the value of parameter *a* also increases. The *c*/*a* ratio, which characterizes tetragonality, decreases (see Table 2) and approaches a value equal to 2, which, according to [12], is ideal tetragonality.

Additionally, we observe a decrease in the half-width of diffraction reflexes after exposure to FLA. Generally, the change in the value of the half-width is influenced by several factors [16, 17]: the change in the size of the regions of coherent scattering and the change in the level of micro-deformations in the material, since the instrumental function for various measurements is the same.

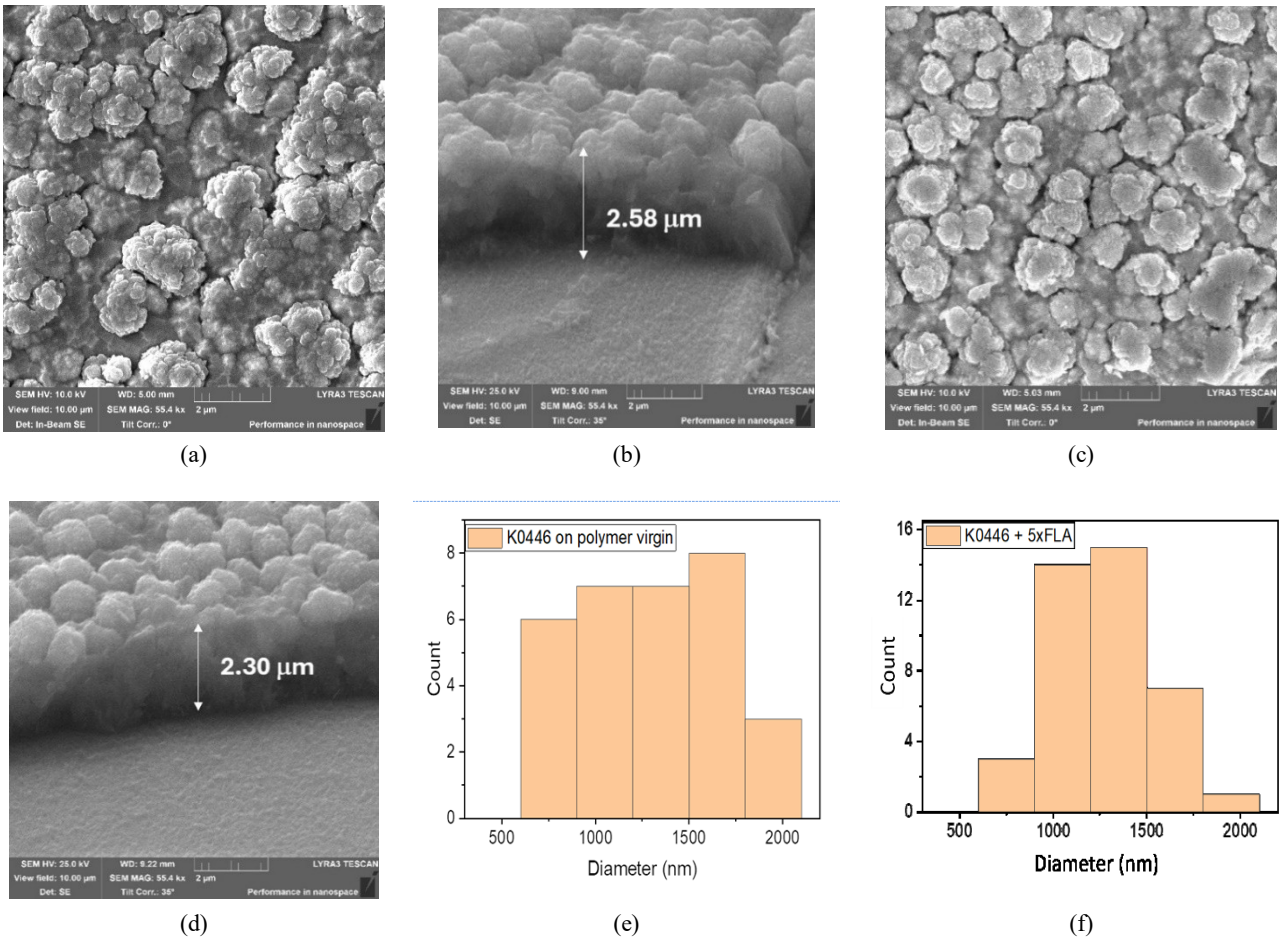

(a) (b) (c)

(d) (e) (f)

Fig. 1. Typical SEM images of the surface (a, c) and cross-section morphology (b, d) of the Cu(InGa)SSe layers on polyimide for initial (a, c) and after FLA with the fluence of 0.627 J/cm^2 (c, d). Statistical analysis of grain size on initial surface (e) and after FLA (f).

Table 1. Chemical composition of the CIGSS films determined using the EDXS technique.

	CIGSS initial	CIGSS after FLA with 0.627 J/cm^2
Element	Atomic %	Atomic %
Se	25.61	25.93
Cu	23.63	24.19
S	22.,07	22.15
In	21.22	20.64
Ga	7.47	7. 09
Cu/(In + Ga)	82	87
Ga/(In + Ga)	26.0	25.6
E_g(eV)	1.152	1.142

Additionally, we observe a decrease in the half-width of diffraction reflexes after exposure to FLA. Generally, the change in the value of the half-width is The well-known Williamson–Hall method [18, 19] allows the separation of these two contributions from the positions and half-widths of several reflexes.

In our case, the reflections of higher orders are too weak and blurred, which does not allow us to use this technique for the obtained diffractograms However, it is possible to estimate the size of coherent scattering regions using Scherer's formula [20]:

$$D = k\lambda/\beta\cos\theta\,, \qquad (1)$$

where D is the size of the coherent scattering regions in nm, λ is the wavelength, β is the half-width of the reflex, parameter k = 0.9, and θ is the angle. The evaluation shows (see Table 2) that the area of coherent scattering is too small compared to the crystallite sizes obtained by scanning electron microscopy.

This may indicate the presence of a significant number of defects and their clusters, which lead to a substantial decrease in the coherence length in the source material. At the same time, an increase in the fluence of FLA leads to an increase in the size of the coherent scattering region by 22%, which indicates a decrease in the defectivity of the structure after FLA.

Micro-strain, ε, was calculated from the following expression [21]:

$$\varepsilon = \frac{\beta\cos\theta}{4}. \qquad (2)$$

Table 2. Lattice parameters and mechanical stresses in the CIGSS lattice after FLA.

E, J/cm^2	2θ reflex (112), degree	Half-width of (112), degree	ε, %	D, nm	Parameter a, Å	Parameter c, Å	c/a
Initial	27.18	0.686	1.19	11.92	5.5631	11.6088	2.086
0.2706	27.16	0.682	1.19	12.11	5.5632	11.6072	2.086
0.3465	27.18	0.675	1.18	12.16	5.5648	11.6009	2.084
0.429	27.16	0.672	1.17	13.22	5.5714	11.5961	2.081
0.5346	27.22	0.618	1.08	13.91	5.5743	11.5852	2.078
0.627	27.25	0.588	1.02	14.58	5.5789	11.5504	2.070

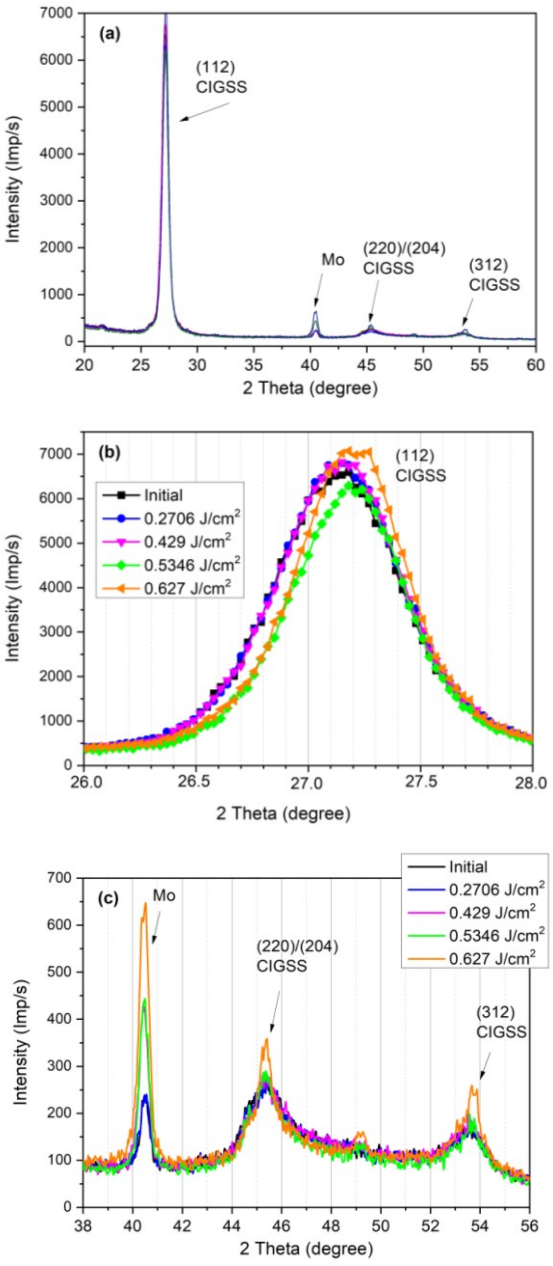

Fig. 2. XRD patterns of CIGSS on PI absorber after FLA treatment. Survey spectra (a), (112) CIGSS reflections (b) and reflections within the range of 38° to 56° (c).

The estimation of the level of micro-deformations using formula (2) (see Table 2) shows a decrease in this value by 14% compared to the initial material. Thus, two effects in the CIGSS structure are observed during every step of FLA. These are: (a) an increase in the size of coherent scattering regions, and (b) a decrease in the level of micro deformations. Observed effects indicate an increase in the structural perfection of the CIGSS layer with each step of FLA. The weak reflexes (220) and (312) (Fig. 2c) become more intense and narrower, which is an additional confirmation of the growth of the structural ordering of CIGSS.

With increasing FLA fluence energy, the intensity of molybdenum reflexes increases starting from the fourth treatment (0.53 J/cm^2), which can be associated with the reduction of the thickness of the CIGSS film. Attention should also be paid to the increase in the concentration of copper, which, in excess, forms an additional crystalline phase of CuSe. The appearance of a peak at 49 degrees in the last two treatments may indicate the formation of a hexagonal CuSe phase, and this peak is probably the (110) reflex of this phase.

3.3. Raman measurements

Fig. 3 shows the Raman spectra of the initial CIGS film and after FLA treatment with the energy fluence of 0.54 J/cm^2. Two vibrational bands close to 190 and 280…290 cm^{-1} were observed. The frequency position of chalcopyrite (CH) A_1 mode for Cu(InGa)Se$_2$ films is usually equal to 175 cm^{-1}[22]. Adding sulfur in the crystalline lattice of the chalcopyrite, in our case, results in a shift of the A_1 mode to 195 cm^{-1}. The weaker peak at 280…290 cm^{-1} can be assigned to the Cu$_x$Se phase or A_1 mode of Cu(InGa)S$_2$ [22, 23]. The shoulder near 150 cm^{-1} can be attributed to chalcopyrite Cu-poor ordered vacancy domains (OVC) [24]. One can see that the FLA leads to insignificant increase in the intensity of A_1 mode of Cu(InGa)SSe and a slight shift of its peak position from 195.3 to 194.9 cm^{-1} due to an increase in the Cu/(Ga + In) ratio [25]. Small increase in the intensity can be associated with a small increase in the size of CH crystallites. The contribution of the Cu$_x$Se phase band becomes more pronounced after FLA treatment.

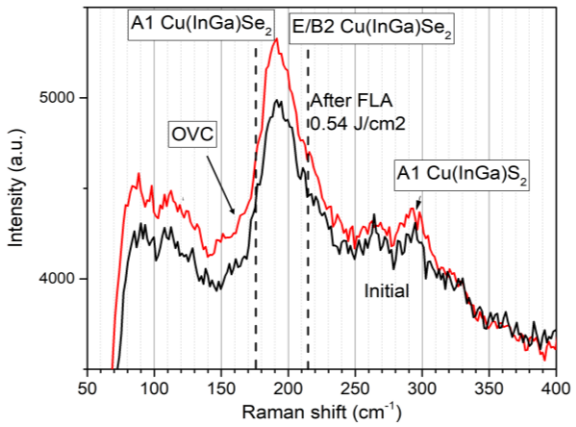

Fig. 3. Raman spectra of the initial CIGS film and after FLA treatment with the energy fluence of 0.54 J/cm^2.

4. Conclusions

We have studied the effect of flash lamp annealing on structural and chemical properties of polycrystalline CIGSS films deposited by the magnetron sputtering technique at low temperature (300 °C) on a polyimide flexible substrate covered by a Mo thin film. It was demonstrated that the FLA resulted in formation of homogeneous polycrystalline material with the grain size close to 1300 nm and an increased Cu concentration. It was shown that FLA leads to reduced defect concentration in the material and an ideal tetragonality of the CH lattice.

Acknowledgements

The authors would like to thank Petro Lytvyn (V. Lashkaryov Institute of Semiconductor Physics, NAS of Ukraine) for help in the analysis of the SEM data. The work was (partially) supported by the Ministry of Education and Science of Ukraine in the frame of the project #M88-2024 and by the Program Science for Peace and Security (NATO project SPS G5853).

References

1. Bonnassieux Y., Brabec C.J., Cao Y. *et al.* The 2021 flexible and printed electronics roadmap. *Flex. Print. Electron*. 2021. **6**. P. 023001. https://doi.org/10.1088/2058-8585/abf986.
2. Green M.A., Dunlop E.D., Yoshita M. *et al.* Solar cell efficiency tables (Version 64). *Prog. Photovolt.: Res. Appl*. 2024. **32**, No 7. P. 425–441. https://doi.org/10.1002/pip.3831.
3. Carron R., Nishiwaki S., Feurer T. *et al.* Advanced alkali treatments for high-efficiency Cu(In,Ga)Se_2 solar cells on flexible substrates. *Adv. Energy Mater*. 2019. **9**, No 24. P. 1900408. https://doi.org/10.1002/aenm.201900408.
4. Constantin C.P., Aflori M., Damian R.F., Rusu R.D. Biocompatibility of polyimides: A mini-review. *Materials*. 2019. **12**. P. 3166. https://doi.org/10.3390/ma12193166.
5. Bremaud D., Rudmann D., Bilger G. *et al.* Towards the development of flexible CIGS solar cells on polymer films with efficiency exceeding 15%. *Conference Record of the Thirty-first IEEE Photovoltaic Specialists Conference, 2005.* 3-7 Jan. 2005, Lake Buena Vista, FL, USA. P. 223–226. https://doi.org/10.1109/PVSC9367.2005.
6. Wu H., Huang Y.A., Yin Z.P. Flexible hybrid electronics: Enabling integration techniques and applications. *Sci. China Technol. Sci.* 2022. **60**, No 9. P. 1995–2006. https://doi.org/10.1007/s11431-022-2074-8.
7. Skorupa W., Schumann T., Rebohle L. Millisecond thermal processing using flash lamps for the advancement of thin layers and functional coatings. *Surf. Coat. Technol.* 2017. **314**. P. 169–176. https://doi.org/10.1016/j.surfcoat.2016.08.010.
8. Kim S.Y., Yoo H., Rana T.R. *et al.* Effect of crystal orientation and conduction band grading of absorber on efficiency of Cu(In,Ga)Se_2 solar cells grown on flexible polyimide foil at low temperature. *Adv. Energy Mater*. 2018. **8**, No 26. P. 1801501. https://doi.org/10.1002/aenm.201801501.
9. Severino N., Bednar N., Adamovic N. Guidelines for optimization of the absorber layer energy gap for high efficiency Cu(In,Ga)Se_2 solar cells. *J. Mater. Sci. Chem. Eng.* 2018. **6**, No 4. P. 147–162. https://doi.org/10.4236/msce.2018.64015.
10. Rietveld H.M. A profile refinement method for nuclear and magnetic structures. *J. Appl. Cryst.* 1969. **2**. P. 65–71. https://doi.org/10.1107/S0021889869006558.
11. Rietveld H.M. The Rietveld method: A retrospection. *Z. Kristallogr*. 2010. 225. P. 545–547. https://doi.org/10.1524/zkri.2010.1356.
12. Balboul M.R., Schock H.W., Fayak S.A. *et al.* Correlation of structure parameters of absorber layer with efficiency of Cu(In, Ga)Se_2 solar cell. *Appl. Phys. A*. 2008. **92**. P. 557–563. https://doi.org/10.1007/s00339-008-4630-z.
13. Albert V. Band gap optimization in $Cu(In_{1-x}Ga_x)(Se_{1-y}S_y)_2$ by controlled Ga and S incorporation during reaction of Cu-(In,Ga) intermetallics in H_2Se and H_2S. *Thin Solid Films*. 2009. **517**. P. 2115–2120. https://doi.org/10.1016/j.tsf.2008.10.127.
14. Liu C.P., Chang M.W., Chuang C.L. The effect of Ga_2Se_3 doping ratios on structure, composition, and electrical properties of $CuIn_{0.5}Ga_{0.5}Se_2$ absorber formed by thermal sintering. *Int. J. Photoenergy*. 2013. **2013**. P. 936364. http://doi.org/10.1155/2013/936364.
15. Koutná N., Holec D., Svoboda O.J. *et al.* Point defects stabilise cubic Mo-N and Ta-N. *J. Phys. D: Appl. Phys*. 2016. **49**. P. 375303. http://doi.org/10.1088/0022-3727/49/37/375303.
16. Saïdi H., Ben Alaya C., Boujmil M.F. *et al.* Physical properties of electrodeposited CIGS films on crystalline silicon: Application for photovoltaic heterojunction. *Curr. Appl. Phys*. 2019. **20**, Issue 1. P. 29–36. https://doi.org/10.1016/j.cap.2019.09.015.

17. Abdulrahman N.A., Haddad N.I.A. Braggs, Scherre, Williamson–Hall and SSP analyses to estimate the variation of crystallites sizes and lattice constants for ZnO nanoparticles synthesized at different temperatures. *NeuroQuantology*. 2020. **18**, No 1. P. 53–63. https://doi.org/10.14704/nq.2020.18.1.NQ20107.
18. Hariyanto B., Wardani D.A.P., Kurniawati N. *et al.* X-ray peak profile analysis of silica by Williamson–Hall and size-strain plot methods. *J. Phys.: Conf. Ser*. 2021. P. 012106. https://doi.org/10.1088/1742-6596/2019/1/012106.
19. Prabhu Y.T., Rao K.V., Kumar V.S.S., Kumari B.S. X-ray analysis by Williamson–Hall and size-strain plot methods of ZnO nanoparticles with fuel variation. *World Journal of Nano Science and Engineering*. 2014. **4**. P. 21–28. http://doi.org/10.1016/j.solidstatesciences.2010.11.024.
20. Patterson A. The Scherrer formula for X-ray particle size determination. *Phys. Rev*. 1939. **56**, No 10. P. 978–982. https://doi.org/10.1103/PhysRev.56.978.
21. Kotbi A., Hartiti B., Fadili S. *et al.* Synthesis and characterization of sprayed CIGS thin films for photovoltaic application. *Mater. Today: Proc*. 2020. **24**, Part 1. P. 66–70. https://doi.org/10.1016/j.matpr.2019.07.537.
22. Palm J., Jost S., Hock R., Probst V. Raman spectroscopy for quality control and process optimization of chalcopyrite thin films and devices. *Thin Solid Films*. 2007. **515**, No 15. P. 5913–5916. https://doi.org/10.1016/j.tsf.2006.12.162.
23. Izquierdo-Roca V., Saucedo E., Ruiz C.M. *et al.* Raman scattering and structural analysis of electrodeposited $CuInSe_2$ and S-rich quaternary $CuIn(S,Se)_2$ semiconductors for solar cells. *phys. status solidi (a)*. 2009. **206**, No 5. P. 1001–1004. https://doi.org/10.1002/pssa.200881239.
24. Izquierdo-Roca V., Fontané X., Álvarez-García J. *et al.* Electrodeposition based synthesis of S-rich $CuIn(S,Se)_2$ layers for photovoltaic applications: Raman scattering analysis of electrodeposited $CuInSe_2$ precursors. *Thin Solid Films*. 2009. **517**, No 7. P. 2163–2166. https://doi.org/10.1016/j.tsf.2008.10.080.
25. Sun L., Ma J., Yao N. *et al.* Copper content dependence of electrical properties and Raman spectra of Se-deficient $Cu(In,Ga)Se_2$ thin films for solar cell. *J. Mater Sci: Mater Electron.* 2016. **27**. P. 9124–9130. https://doi.org/10.1007/s10854-016-4947-x.

Authors' contributions

Tyagulski I.P.: formal analysis, investigation, data curation, visualization, writing – original draft.
Gudymenko O.Yo.: formal analysis, investigation, data curation, visualization, writing – original draft.
Rusavsky A.V.: investigation, resources, methodology, writing – original draft.
Tiagulskyi S.I.: formal analysis, investigation, data curation, visualization, writing – original draft.
Isaieva O.F.: formal analysis, investigation, data curation, visualization, writing – original draft.
Kondratenko S.V.: formal analysis, investigation, data curation, visualization, writing – original draft.
Lysenko V.S.: conceptualization, methodology, writing – original draft.
Flandre D.: conceptualization, methodology, project administration, writing – review & editing.
Nazarov A.N.: conceptualization, methodology, data curation, validation, formal analysis, funding acquisition, writing – original draft.

Authors and CV

Igor P. Tyagulskyy, PhD, Senior Researcher at the Diagnostic Center "Diagnostics of semiconductor materials, structures and devices", V. Lashkaryov Institute of Semiconductor Physics. Authored over 160 publications. The area of his scientific interests as follow: electronic processes in transition layers of Si-SiO_2, SiC-SiO_2, SiC-Si structures at cryogenic temperatures, low temperature characterization of MOS(SOI) FET's. E-mail: tyag969@gmail.com, https://orcid.org/0009-0002-6832-6544

Olexandr Yo. Gudymenko, PhD, Senior Researcher at the Department of Ion-Beam Engineering, V. Lashkaryov Institute of Semiconductor Physics. Author of more than 60 publications. Field of research: solid-state physics, dynamical theory of diffraction of radiation, X-ray optics, X-ray diffraction analysis of semiconductor crystals. E-mail: gudymen@ukr.net, https://orcid.org/0000-0002-5866-8084

Andrii V. Rusavsky, PhD, Senior Researcher at the V. Lashkaryov Institute of Semiconductor Physics. Author of more than 40 publications. Research interests: development of deposition technology (ion sputtering at direct current and RF-current) and the production of thin amorphous films of carbon, silicon, germanium, composite materials based on ZnO. E-mail: rusavsky@yahoo.com, https://orcid.org/0000-0001-6386-3434

Stanislav Tiagulskyi, PhD in Semiconductor and Dielectric Physics (V. Lashkaryov Institute of Semiconductor Physics). He joined the 'Synthesis and Characterization of Nanomaterials' Group at the Institute of Photonics and Electronics, Czech Academy of Sciences in 2017. Since then, he specialized in research on the electrical properties of wide bandgap semiconductor nanostructures, including in-situ SEM IV characterization of individual semiconductor nanowires. https://orcid.org/0000-0002-3266-3947, e-mail: tiagulskyi@ufe.cz

Oksana F. Isaieva, PhD in Applied Physics and Nanomaterials, Researcher at the V. Lashkaryov Institute of Semiconductor Physics. Author of more than 20 publications, 7 patents. The area of her scientific interests includes nanocomposites and their synthesis, optical properties of nanomaterials.
E-mail: oksana.isaieva@isp.kiev.ua,
https://orcid.org/0000-0003-1313-5409

Serhiy V. Kondratenko, Doctor of Sciences in Physics and Mathematics, Professor, Head of Optics Division, Faculty of Physics, Taras Shevchenko National University of Kyiv. Author of more than 80 publications. Research interests: semiconductor heterostructures and nanostructures, solar cells, optical and photoelectric properties of semiconductors. https://orcid.org/0000-0002-4403-7732, e-mail: kondratenko@knu.ua

Volodumyr Lysenko, Doctor of Sciences in Physics of Semiconductors and Dielectrics, Corresponding Member of the NAS of Ukraine, Chief Researcher at the V. Lashkaryov Institute of Semiconductors Physics, NASU. His research areas are micro-, nano-, opto-electronics, information technologies, and nanoparticles for antiviral and anticancer therapy. Authored 5 monographs and more than 350 scientific papers. http://orcid.org/0000-0001-9948-9499

Denis Flandre, Full-time Professor in Electronics at UCLouvain, Member of several EU Networks of Excellence on High-Temperature Electronics, SOI Technology, and Nanoelectronics and Micro- Nanotechnology and is an Active Member of the SOI Industry Consortium and EUROSOI Network. He is involved in the research and development of advanced semiconductor devices, digital and analog circuits, as well as sensors and photovoltaic cells. He has authored or co-authored more than 1000 scientific articles or conference contributions and 14 patents.
E-mail: denis.flandre@uclouvain.be,
https://orcid.org/0000-0001-5298-5196

Alexei (Oleksiy) Nazarov, Doctor of Sciences in Physics and Mathematics, Professor, Head of Department at the V. Lashkaryov Institute of Semiconductor Physics, NAS of Ukraine; Professor of Department of General Physics and Modelling of Physical Processes; Faculty of Physics and Mathematics, Igor Sikorsky National Technical University of Ukraine (KPI). Author of more than 250 publications. Research interests: physics, technology and electrical diagnostics of modern nanoscale carbon structures such as graphene, graphene oxide, carbon nanodots.
E mail: nazarov@lab15.kiev.ua,
https://orcid.org/0000-0002-1823-8290

Ламповий відпал плівок $Cu(In_{1-x}Ga_x)SSe$, нанесених на поліімідну підкладку: кристалічна структура та хімічний склад

І.П. Тягульський, О.Йо. Гудименко, А.В. Русавський, С.І. Тягульський, О.Ф. Ісаєва, С.В. Кондратенко, В.С. Лисенко, D. Flandre, А.Н. Назаров

Анотація. У цій статті досліджено вплив відпалу спалаховою лампою (FLA) субмілісекундного діапазону на мікроструктуру та хімічний склад плівок $Cu(In_{1-x}Ga_x)SSe$ (CIGSS), нанесених при низькій температурі (нижчій за 350 °C) на гнучкий поліімід. Результати скануючої електронної мікроскопії (SEM), дифракції рентгенівських променів (XRD), мікро-Раманівської спектроскопії показують, що відпал спалаховою лампою приводить до більш однорідної полікристалічної структури та зменшує концентрацію дефектів у шарі CIGSS. Крім того, енергодисперсійні рентгенівські спектроскопічні (EDS) вимірювання показують, що концентрація міді дещо збільшується з незначним зниженням концентрації Ga та In.

Ключові слова: спалаховий ламповий відпал, скануюча електронна мікроскопія, рентгенівська дифракція, мікрораманівська спектроскопія.